Biodegradation (2007) 18:123–131
DOI 10.1007/s10532-006-9048-8

Degradation of phenanthrene by *Burkholderia* sp. C3: initial 1,2- and 3,4-dioxygenation and *meta*- and *ortho*-cleavage of naphthalene-1,2-diol

Jong-Su Seo, Young-Soo Keum, Yuting Hu, Sung-Eun Lee & Qing X. Li*
*Department of Molecular Biosciences and Bioengineering, University of Hawaii, Honolulu, Hawaii 96822, USA (*author for correspondence: e-mail: qingl@hawaii.edu)*

Accepted 24 January 2006

Key words: 2-carboxycinnamic acid, biodegradation, *Burkholderia*, *meta*-cleavage, *ortho*-cleavage, phenanthrene

Abstract

Burkholderia sp. C3 was isolated from a polycyclic aromatic hydrocarbon (PAH)-contaminated site in Hilo, Hawaii, USA, and studied for its degradation of phenanthrene as a sole carbon source. The initial 3,4-C dioxygenation was faster than 1,2-C dioxygenation in the first 3-day culture. However, 1-hydroxy-2-naphthoic acid derived from 3,4-C dioxygenation degraded much slower than 2-hydroxy-1-naphthoic acid derived from 1,2-C dioxygenation. Slow degradation of 1-hydroxy-2-naphthoic acid relative to 2-hydroxy-1-naphthoic acid may trigger 1,2-C dioxygenation faster after 3 days of culture. High concentrations of 5,6- and 7,8-benzocoumarins indicated that *meta*-cleavage was the major degradation mechanism of phenanthrene-1,2- and -3,4-diols. Separate cultures with 2-hydroxy-1-naphthoic acid and 1-hydroxy-2-naphthoic acid showed that the degradation rate of the former to naphthalene-1,2-diol was much faster than that of the latter. The two upper metabolic pathways of phenanthrene are converged into naphthalene-1,2-diol that is further metabolized to 2-carboxycinnamic acid and 2-hydroxybenzalpyruvic acid by *ortho*- and *meta*-cleavages, respectively. Transformation of naphthalene-1,2-diol to 2-carboxycinnamic acid by this strain represents the first observation of *ortho*-cleavage of two rings-PAH-diols by a Gram-negative species.

Introduction

Polycyclic aromatic hydrocarbons (PAHs) are ubiquitous environmental contaminants derived from both natural and human activities, many of which have been concerned over their toxic, carcinogenic, and mutagenic properties. Interest in the biodegradation mechanisms and environmental fate of PAH is motivated by their ubiquitous distribution, low bioavailability, high persistence, and their potentially deleterious effect on environmental and human health (Johnsen et al. 2005).

Many bacterial species capable of PAH degradation have been isolated and belong to the genera of *Arthrobacter* (Samanta et al. 1999), *Pseudomonas* (Balashova et al. 1999), *Rhodococcus* (Dean-Ross et al. 2002), *Mycobacterium* (Dean-Ross et al. 2002; Kim et al. 2005; Moody et al. 2001), *Sphingomonas* (Pinyakong et al. 2000; van Herwijnen et al. 2003), and *Stenotrophomonas* (Juhasz et al. 2000). In addition, *Burkholderia* sp. are well known to degrade various environmental contaminants such as 2,4-dinitrotoluene (Johnson et al. 2000), polychlorobiphenyls (Camara et al. 2004), trichloroethylene (Canada et al. 2002), and PAHs (Balashova et al. 1999; Juhasz et al. 1997; Kang et al. 2003; Kim et al. 2003). Degradation of phenanthrene by bacteria has been reported (Balashova et al. 1999; Kang et al. 2003; Kim et al. 2005; Moody et al. 2001; Pinyakong et al. 2000; Samanta et al. 1999). However, detailed degradation pathways of phenanthrene by *Burkholderia* are limited. In

general, phenanthrene is metabolized from an initial 3,4-dioxygenation, and after several additional biochemical reactions, 1-hydroxy-2-naphthoic acid is formed. 1-Hydroxy-2-naphthoic acid is further degraded either through salicylic acid and catechol or through phthalic acid and protocatechuic acid according to the bacterial species (Prabhu & Phale 2003; Stingley et al. 2004). There were few studies of initial dioxygenation at the 1,2-position of phenanthrene by Gram-negative bacteria. Although Pinyakong et al. (2000) suggested that *Sphingomonas* sp. strain P2 dioxygenated phenanthrene at 1,2-C positions to produce salicylic acid through 2-hydroxy-1-naphthoic acid, 2-hydroxy-1-naphthoic acid was not detected. Moody et al. (2001) reported that the dioxygenation and monooxygenation at 9,10-positions of phenanthrene yielded *cis*- and *trans*-9,10-dihydroxy-9,10-dihydrophenanthrene, respectively. In this study, we focused on catabolic pathways of phenanthrene by *Burkholderia* sp. C3. To our knowledge, this is the first detailed study of phenanthrene catabolism by *Burkholderia* sp.

Materials and methods

Chemicals

Phenanthrene (>98% purity), 2-hydroxy-1-naphthoic acid, 1-hydroxy-2-naphthoic acid, naphthalene-1,2-diol, coumarin, 2-carboxycinnamic acid, salicylic acid, phthalic acid, and gentisic acid were purchased from Sigma-Aldrich (Milwaukee, WI) or TCI America (Portland, OR). All chemicals used for media were at least reagent grade. All organic solvents used were of high performance liquid chromatography (HPLC) grade and purchased from Fisher Scientific (Pittsburgh, PA). 5,6- and 7,8-Benzocoumarin and 2-hydroxybenzalpyruvic acid that were not commercially available were previously synthesized (Keum et al. 2005).

Isolation and identification of PAH-degrading bacteria

A PAHs-contaminated soil sample was collected from Hilo, Hawaii (Keum et al. 2006 in press). Thirteen of the 16 EPA priority PAHs were detected, and the concentrations of each varied from 0.6 to 30 mg kg^{-1} dry weight, whereas naphthalene, fluorene, and dibenz[*a,h*]anthracene were not detected (data not shown). Several PAH metabolites including acenaphthenone, phthalic acid, gentisic acid, protocatechuic acid, *o*-hydroxynaphthoic acids, diphenic acid, naphthalene-1,2-dicarboxylic acid, 9-fluorenone-1-carboxylic acid, and phenanthrene-4,5-dicarboxylic acid were also detected in the soil sample. Strain C3 was isolated from the soil via soil enrichment cultures in minimum medium (MM) supplemented with phenanthrene crystals (50 mg in 50 ml MM). Taxanomic entity of strain C3 was identified by 16S rDNA. Genomic DNA was extracted with a mixture of phenol and chloroform (Marmur 1961). A fragment of the 16S rRNA gene was amplified from the genomic DNA (100–200 ng μl^{-1}) by polymerase chain reaction (PCR) with 1.25 U of *Taq* DNA polymerase (Takara Mirus Bio, Inc., Madison, WI) and 0.5 μM each of primers 27F and 1492R (Lane 1991). Amplification was performed with a Techne thermal cycler (Techne, Inc., Burlington, NJ) as follows: an initial step at 95 °C for 4 min followed by 30 cycles of 95 °C for 1 min, 55 °C for 50 s and 72 °C for 1.5 min, and a final elongation step at 72 °C for 7 min. The product was purified with the Ultraclean PCR purification kit (Mo Bio Lab, Inc., Carlsbad, CA), and sequenced in both directions using an Applied Biosystems 377XL DNA sequencer. 16S rDNA sequences were manually edited and assembled in Sequencher and Seqman (DNASTAR). Assembled sequences were compared with those in the public domain through a BLASTn search (Altschul et al. 1997). The 16S rRNA analysis showed that strain C3 was the most close to *Burkholderia* sp. 56 (AY177370) with 99% similarity. The 16S rRNA gene sequence (1411 bp) of strain C3 was deposited to GenBank named as *Burkholderia* sp. C3 (AY943387).

Biodegradation kinetics of phenanthrene

The bacterial cells were pre-grown in phenanthrene-supplemented MM (Bastiaens et al. 2000) to an optical density of 0.2 at 540 nm. A 200-μl of phenanthrene solution (1000 mg l^{-1} in acetone) was placed into a sterilized culture tube. After the solvent was evaporated with nitrogen gas, MM (4 ml) and pre-grown cells (1 ml) were added. The culture tube was incubated at 28 °C, 150 rpm in the dark for various time intervals, and extracted with ethyl acetate (5 ml) for determination of phenan-

threne degradation. Also, bacterial growth was monitored by measuring optical density at 540 nm using a Cary 50 Bio spectrophotometer (Varian Inc., CA). Cultures inoculated with boiled dead cells were controls. All experiments were carried out in triplicates.

Growth of bacterium and extraction of metabolites

Strain C3 was grown in MM supplemented with phenanthrene (500 mg in 1.5 l) as a sole source of carbon and energy at 28 °C and 150 rpm (C24 Rotary shaker, New Brunswick Scientific, NJ). Cultures were also done with 1-hydroxy-2-naphthoic acid or 2-hydroxy-1-naphthoic acid (200 mg l^{-1}).

After incubation for 3, 7, 9, and 14 days, the cultures were filtered through glass wool followed by centrifugation (6000×*g*, 10 min) to remove the unreacted crystalline phenanthrene, if any left, and bacterial cells. The pellet was discarded. The supernatant was acidified to pH 2.3 with 6 N HCl, and then extracted with ethyl acetate (3×500 ml). The combined organic layer was extracted with aqueous sodium hydroxide (NaOH 10 mM, 3×500 ml). The remaining organic phase was dried over anhydrous sodium sulfate and concentrated to 5 ml (neutral fraction). The aqueous NaOH extracts were acidified to pH 2.3, and then extracted with ethyl acetate (3×500 ml) (acidic fraction).

Metabolites in the neutral fraction after derivatization or no derivatization were analyzed with a gas chromatograph–mass spectrometer (GC-MS). After removal of ethyl acetate from the neutral fraction, the residue was dissolved in acetone (10 ml) followed by addition of 50 mg of *n*-butylboronic acid. After refluxing for 30 min, the mixture was concentrated to 1 ml and analyzed by GC-MS. Diols and *cis*-dihydrodiols in the residue were derivatized with diazomethane and re-analyzed with GC-MS (Keum et al. 2006 in press). Metabolites in the acidic fraction were also derivatized with diazomethane and detected with GC-MS.

Analytical methods

GC-MS analyses were performed on a Varian QP-5000 gas chromatograph with Saturn-2000 mass spectrometer (Varian Inc., Palo Alto, CA), equipped with ZB-1 column (60 m, 0.25 μm film thickness, Phenomenex, Inc., Torrance, CA). The carrier gas was helium at a rate of 2 ml min^{-1}. The column temperature started from 120 °C (2 min), increased to 280 °C at a rate of 2 °C min^{-1}, and was held at 280 °C for 10 min. Injector and analyzer temperatures were 270 and 280 °C, respectively. The mass spectrometer was at electron impact mode (70 eV).

Results

Phenanthrene (40 mg l^{-1}) was completely degraded by *Burkholderia* sp. C3 in 7 days as compared with no phenanthrene degradation in the sterilized controls (Figure 1). The results showed that the bacterial growth was related to phenanthrene available in the culture medium. Bacterial cell densities started to decrease on day 5 of culture as phenanthrene was almost completely utilized. The cell densities decreased approximately 30% of the maximum density on day 7 of culture as phenanthrene was completely utilized. A total of 13 phenanthrene metabolites were detected in culture supernatants and identified by the comparison of their mass spectra and GC retention times (*Rt*) with those of authentic standards (Table 1). Kinetic profiles of phenanthrene catabolism are shown in Figure 2. Ten of the 13 metabolites were detected in the acidic fraction. Two benzocoumarins (P3 and P4; *Rt*, 41.75 and 39.52 min) were detected and identified as 5,6- and 7,8-benzocoumarin having a molecular ion (M^+) at *m*/*z* 196 and fragment ions at *m*/*z* 168 (M^+—CO) and 139 (M^+—CO—CHO) (Table 1). This fragmentation pattern was the same as that obtained by Pinyakong et al. (2000). Both metabolites P3 and P4 peaked at day 7 and 3, respectively. However, they were not detected after 9-day incubation (Figure 2b). Two hydroxynaphthoic acids (P5 and P6) were confirmed with their methyl ester derivatives (Table 1). The losses of fragment ions for hydroxynaphthoic acid methyl esters (P5 and P6) differed from typical losses for the methyl derivatives of P11 and P13 (Table 1). However, the mass spectral fragmentation patterns and GC retention times of P5 and P6 were identical to those of the authentic standards and the same as the results of Pinyakong et al. (2000). Therefore, P5 and P6 were 2-hydroxy-1-naphthoic acid and 1-hydroxy-2-naphthoic acid, respectively.

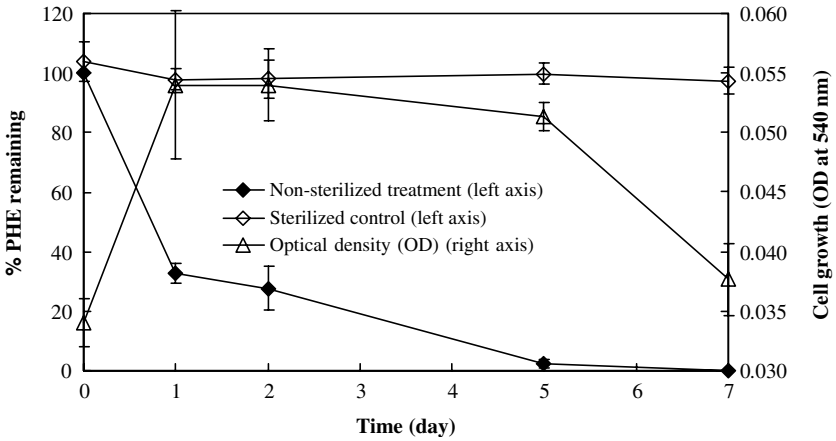

Figure 1. Degradation kinetics of phenanthrene (PHE) by *Burkholderia* sp. C3 and its growth in minimum medium supplemented with phenanthrene at 40 mg l^{-1}. The error bars represent the standard deviations of triplicates.

Table 1. Identification of phenanthrene metabolites by comparison of their GC-MS retention times and mass spectra to those of authentic standards

ID	Name[a]	Retention time (min)	MS fragmentation pattern[b]
P1[c]	*cis*-Phenanthrene-1,2-dihydrodiol (BuB)	53.47	278 (M^+, 100), 221 (29), 194 (75), 178 (14)
P2[c]	*cis*-Phenanthrene-3,4-dihydrodiol (BuB)	50.83	278 (M^+, 100), 221 (11), 194 (20), 177 (17)
P3	5,6-Benzocoumarin	41.75	196 (M^+, 70), 168 (100), 139 (54)
P4	7,8-Benzocoumarin	39.52	196 (M^+, 61), 168 (100), 139 (54)
P5	2-Hydroxy-1-naphthoic acid (Me)	28.95	202 (M^+, 57), 170 (100), 142 (53), 114 (44)
P6	1-Hydroxy-2-naphthoic acid (Me)	28.67	202 (M^+, 48), 170 (100), 142 (16), 114 (69)
P7	Naphthalene-1,2-diol (BuB)	33.40	226 (M^+, 39), 170 (100)
P8	Coumarin	14.67	146 (M^+, 68), 118 (100), 89 (45)
P9	2-Hydroxybenzalpyruvic acid (diMe)[d]	34.28	220 (M^+, 7), 205 (1), 189 (1), 161 (100)
P10	2-Carboxycinnamic acid (diMe)	28.41	220 (M^+, 5), 205 (1), 189 (13), 161 (100)
P11	Salicylic acid (Me)	7.98	152 (M^+, 66), 137 (2), 120 (100), 92 (78)
P12	Phthalic acid (diMe)	15.39	194 (M^+, 1), 163 (100)
P13	Gentisic acid (Me)	18.73	168 (M^+, 65), 153 (1), 136 (100), 108 (47)

[a]Derivatives of: BuB, *n*-butylboronic acid; Me, methyl ester; diMe, dimethyl ester.
[b]Values in paranthesis represent m/z of molecular ion (M^+) and relative abundance.
[c]P1 and P2 were tentatively identified by comparison of their GC-MS mass spectra with those reported by Krivobok et al. (2003).
[d]Detected as 2-methoxybenzalpyruvic acid methyl ester.

1-Hydroxy-2-naphthoic acid (P6) accumulated throughout the entire 14-day incubation. However, 2-hydroxy-1-naphthoic acid (P5) had a maximum concentration at day 7 and disappeared after 9-day incubation (Figure 2c). Metabolite P8 (*Rt*, 14.67 min) had a molecular ion (M^+) at m/z 146 and fragment ions at m/z 118 (M^+—CO) and 89 (M^+—CO—CHO), and was identified as coumarin (Table 1). Its concentration reached to maximum at day 7 and then declined rapidly to undetectable at day 9 (Figure 2d). 2-Hydroxybenzalpyruvic acid (P9) and 2-carboxycinnamic acid (P10) derived from naphthalene-1,2-diol gave mass spectra and GC retention times identical to those of the standard 2-methoxybenzalpyruvic acid methyl ester (*Rt*, 34.28 min) and 2-carboxycinnamic acid dimethyl ester (*Rt*, 28.41 min), respectively, both having a molecular ion (M^+) at m/z 220 and fragment ions at m/z 205 (M^+—CH_3), 189 (M^+—OCH_3), and 161 (M^+—OCH_3—CO) (Table 1). This fragmentation pattern is similar with the result of Annweiler et al. (2000). The concentration of P9 reached maximum at day 7 and completely disappeared after 9 days of

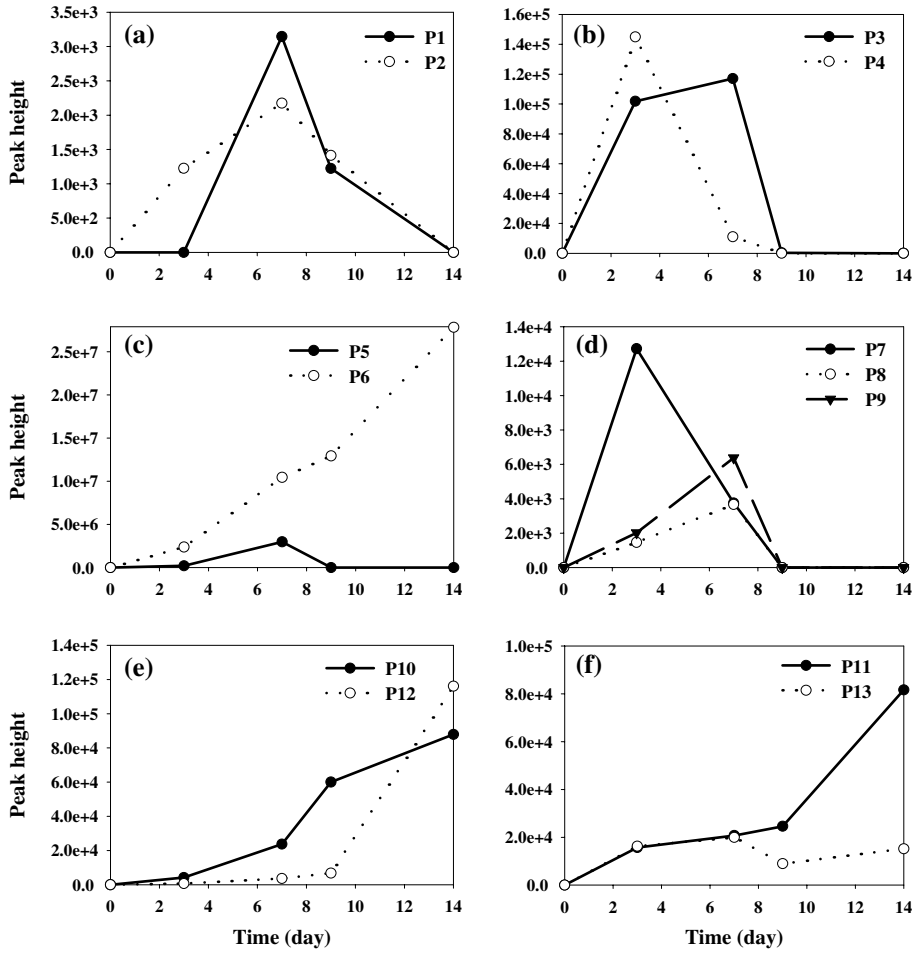

Figure 2. Kinetics of phenanthrene catabolism and its metabolite profiles. *cis*-Phenanthrene-1,2-dihydrodiol (P1) and *cis*-phenanthrene-3,4-dihydrodiol (P2) (a), 5,6-benzocoumarin (P3), and 7,8-benzocoumarin (P4) (b), 2-hydroxy-1-naphthoic acid (P5) and 1-hydroxy-2-naphthoic acid (P6) (c), naphthalene-1,2-diol (P7), coumarin (P8), and 2-hydroxybenzalpyruvic acid (P9) (d), 2-carboxycinnamic acid (P10) and phthalic acid (P12) (e), and salicylic acid (P11) and gentisic acid (P13) (f). Phenanthrene in bacteria-free cultures remained unreacted for 14 days.

incubation (Figure 2d). However, the concentrations of P10 increased gradually up to 14 days of incubation (Figure 2e). Metabolites P11 and P13 were detected as their monomethyl derivatives, and were salicylic acid methyl ester [m/z 152 (M^+), 137 (M^+—CH_3), 120 (M^+—CH_3—OH), 92 (M^+—CH_3—COOH)] at *Rt* 7.98 min and gentisic acid methyl ester [m/z 168 (M^+), 153 (M^+—CH_3), 136 (M^+—CH_3—OH), 108 (M^+—CH_3—COOH)] at *Rt* 18.73 min, respectively (Table 1). The concentrations of P11 gradually increased to maximum at day 14 (Figure 2f). The concentrations of P13 remained fairly constant throughout the entire incubation period (Figure 2f). Metabolite P12 (*Rt*, 15.39 min) was identified with its dimethylated derivative, phthalic acid dimethyl ester, which had a molecular ion (M^+) at m/z 194 and fragment ion at m/z 163 (M^+—OCH_3) (Table 1). Its concentrations remained very low at and before day 9, and increased exponentially from day 9 to day 14 (Figure 2e).

Three metabolites were detected and identified in the neutral fraction. Among several common dihydrodiols from bacterial metabolism of phenanthrene, two *cis*-phenanthrene dihydrodiols (P1 and P2) derivatized with *n*-butylboronate were found at 53.47 and 50.83 min. Mass spectra of the two metabolites [m/z 278 (M^+), 221 (M^+—$(CH_2)_3$—CH_3), 194 (M^+—$(CH_2)_3$—CH_3—BO), 178 (M^+—$(CH_2)_3$—CH_3—BO—O)] were very similar

with the results of Krivobok et al. (2003). From these results, the two phenanthrene dihydrodiols P1 and P2 were tentatively identified as *cis*-phenanthrene-1,2-dihydrodiol and *cis*-phenanthrene-3,4-dihydrodiol (Table 1), respectively. The concentrations of the two metabolites reached maximum at after 7-day incubation. P1 was not detected at day 3, but the concentration of P2 was quite high at day 3 (Figure 2a). This result suggested that the initial dioxygenation started at 3,4-C positions of phenanthrene followed by rapid dioxygenation at 1,2-C positions. Metabolite P7 was also detected as *n*-butylboronate derivative having a molecular ion (M^+) at *m*/*z* 226 and fragment ion at *m*/*z* 170 (M^+—CH—CH2—CH2—CH_3) and identified as naphthalene-1,2-diol (Table 1). During the entire incubation period, P7 was detected only at 3 day (Figure 2d).

Careful analysis of the neutral fractions extracted from the separate cultures of 1-hydroxy-2-naphthoic acid (P6) and 2-hydroxy-1-naphthoic acid (P5) as initial substrates in two identical experiments showed that the amount of naphthalene-1,2-diol varied largely (Figure 3). The concentration of naphthalene-1,2-diol derived from 2-hydroxy-1-naphthoic acid (Figure 3b) was approximately 4 times higher than that from 1-hydroxy-2-naphthoic acid (Figure 3a). This result supported the constant accumulation of 1-hydroxy-2-naphthoic acid (P6) throughout the incubation (Figure 2c). In other words, 1-hydroxy-2-naphthoic acid (P6) is more difficult to be degraded than 2-hydroxy-1-naphthoic acid (P5) by *Burkholderia* sp. C3. Slow degradation of 1-hydroxy-2-naphthoic acid (P6) relative to 2-hydroxy-1-naphthoic acid (P5) may trigger 1,2-C dioxygenation faster.

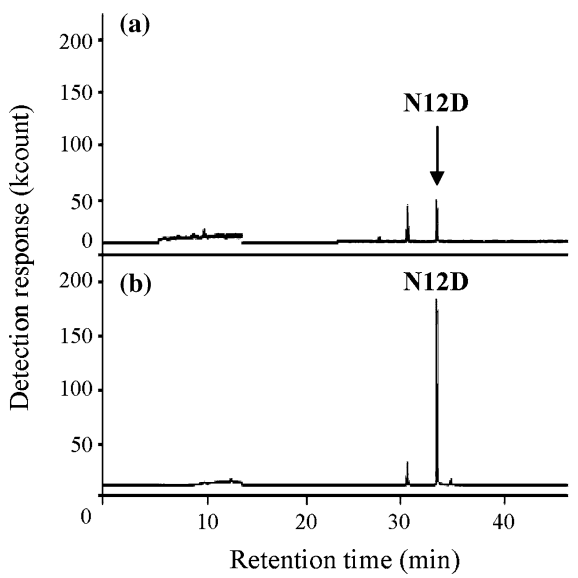

Figure 3. GC-MS chromatograms of neutral extraction fractions from the two identical replacement cultures of *Burkholderia* sp. C3, treated with 1-hydroxy-2-naphthoic acid (a) or 2-hydroxy-1-naphthoic acid (b) after 7 days of incubation. N12D, naphthalene-1,2-diol as its *n*-butylboronate ester. 1-Hydroxy-2-naphthoic acid and 2-hydroxy-1-naphthoic acid in bacteria-free cultures remained unreacted for 7 days.

Discussion

The identification of dioxygenation and ring cleavage products revealed that *Burkholderia* sp. C3 can decompose phenanthrene through two upper (from PHE to P7) and two lower (from P7 to P12 and P13) degradation pathways (Figure 4). Catabolic pathways were proposed based on the metabolites that were identified by comparison of their mass spectra and GC retention times with those of authentic standards (Figure 4). Phenanthrene degradation by *Burkholderia* sp. C3 was initiated by dioxygenation at 1,2-C and 3,4-C positions of phenanthrene to form *cis*-phenanthrene-1,2-dihydrodiol (P1) and *cis*-phenanthrene-3,4-dihydrodiol (P2), respectively. This suggested either diverse dioxygenase systems or/and a dioxygenase system with broad specificity (e.g., relaxed regiospecificity) (Gibson & Parales 2000; Parales et al. 2000). P2 was further metabolized to 1-hydroxy-2-naphthoic acid (P6) through phenanthrene-3,4-diol (I2) presumably by dihydrodiol dehydrogenase, 4-(1-hydroxy-2-naphthyl)-2-oxobut-3-enoic acid (I4) via *meta*-cleavage, and 1-hydroxy-2-naphthaldehyde (I6) presumably by hydratase-aldolase. This pathway is similar with that proposed by Stingley et al. (2004). Being similar to P2, P1 was metabolized to 2-hydroxy-1-naphthoic acid (P5) through phenanthrene-1,2-diol (I1), 4-(2-hydroxy-1-naphthyl)-2-oxobut-3-enoic acid (I3), and 2-hydroxy-1-naphthaldehyde (I5). The two hydroxy naphthoic acids (P5 and P6) undergo enzymatic de-carboxylation and hydroxylation to naphthalene-1, 2-diol (P7). Balashova et al. (2001) purified a monooxygenase, which catalyzed the oxidation of 1-hydroxy-2-naphthoic acid (P6) to

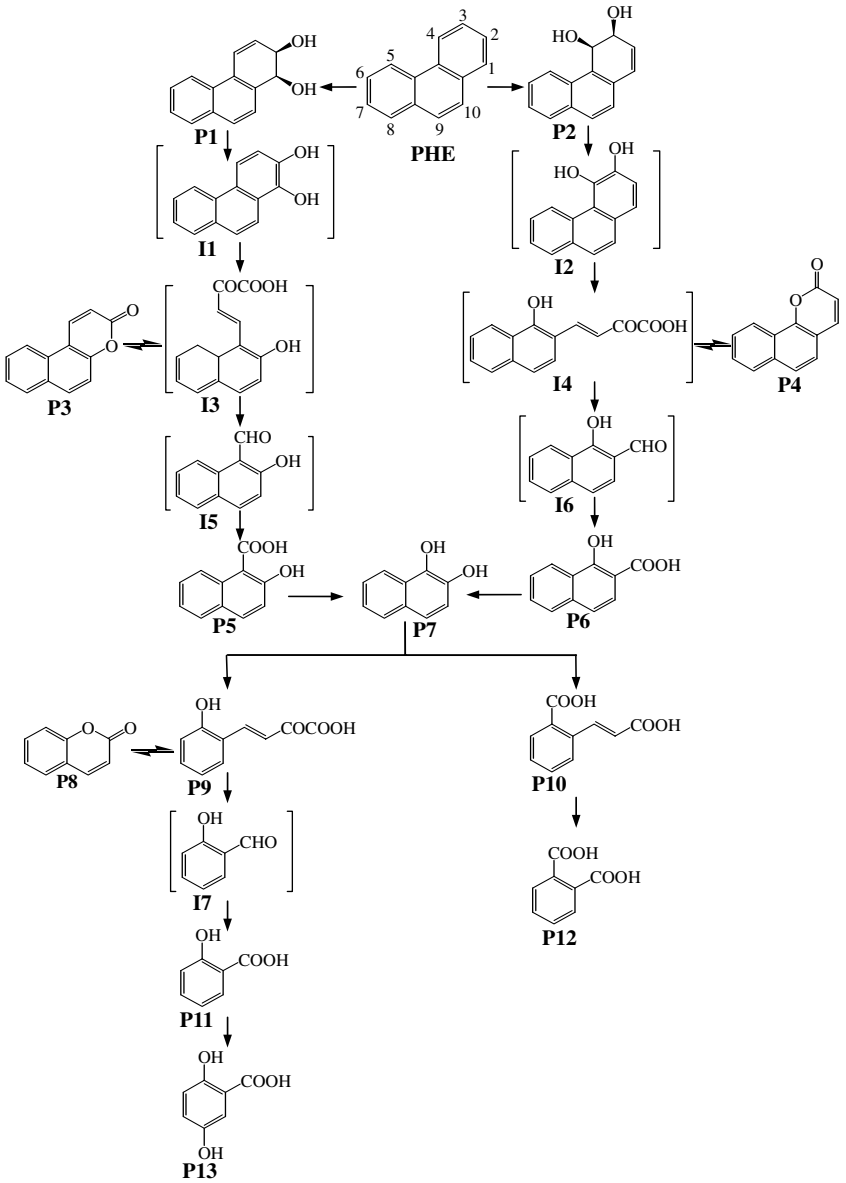

Figure 4. Proposed catabolic pathways of phenanthrene by *Burkholderia* sp. C3. P1 to P13 are described in Table 1. Metabolites in brackets are proposed structures, but not detected. I1, phenanthrene-1,2-diol; I2, phenanthrene-3,4-diol; I3, 4-(2-hydroxy-1-naphthyl)-2-oxobut-3-enoic acid; I4, 4-(1-hydroxy-2-naphthyl)-2-oxobut-3-enoic acid; I5, 2-hydroxy-1-naphthaldehyde; I6, 1-hydroxy-2-naphthaldehyde; and I7, salicylic aldehyde.

1,2-dihydroxynaphthalene (P7), from phenanthrene degrading *Pseudomonas putida* strain BS202-P1. We found two benzocoumarins, 5,6-benzocoumarin (P3) and 7,8-benzocoumarin (P4), which were well-known metabolites from the rearrangement of *o*-hydroxynaphthyl-α-oxobutenoates (I3 and I4) (Pinyakong et al. 2000). The identification of metabolites P3 and P4 also supported the initial dioxygenation at both 1,2-C and 3,4-C positions of phenanthrene followed by *meta*-cleavage as the catabolic mechanisms to yield naphthalene-1,2-diol (P7) observed in the upper pathways.

In two upper pathways from phenanthrene dihydrodiols to naphthalene-1,2-diol, the initial dioxygenation at 3,4-C positions might be dominant in the first 3 days of incubation because the concentrations of P2 and P4 were higher than

those of P1 and P3 during the initial incubation (Figure 2a, b). However, P1 and P3 were more abundant than P2 and P4, respectively, at day 7. The results indicated an interrelationship between the 1,2-dioxygenation and 3,4-dioxygenation pathways. Hydroxy naphthoic acids have been well recognized to be major transformation products of phenanthrene. Balashova et al. (1999) reported that the major intermediates of phenanthrene metabolism accumulated in the culture liquid were 1-hydroxy-2-naphthoic acid (P6) and 2-hydroxy-1-naphthoic acid (P5). We also found a constant accumulation of 1-hydroxy-2-naphthoic acid (P6) in the phenanthrene-supplemented media where the strain C3 grew throughout the 14-day incubation period (Figure 2c). 2-Hydroxy-1-naphthoic acid (P5), however, did not accumulate (Figure 2c), which suggested that degradation of P5 be not a limiting step. The replacement culture tests with P5 or P6 as an initial substrate clearly showed rapid degradation of P5 and accumulation of P6 that was derived from 3,4-dioxygenation, which suggested that slow degradation of P6 probably facilitated 1,2-dioxygenation (Figure 3). Two upper metabolic pathways of phenanthrene are converged into naphthalene-1,2-diol (P7) (Figure 4).

Naphthalen-1,2-diol (P7) was further degraded through *meta*- and *ortho*-cleavages. *meta*-Cleavage of P7 yielded 2-hydroxybenzalpyruvic acid (P9), which was then transformed to gentisic acid (P13) through salicylic aldehyde (I7) and salicylic acid (P11) presumably catalyzed by hydratase-aldolase and dehydrogenase, respectively (Eaton & Chapman 1992). This pathway involving hydratase–aldolase has been studied in the phenanthrene and naphthalene metabolism by *Sphingomonas* sp. strain P2 (Pinyakong et al. 2000) and *Bacillus thermoleovorans* (Annweiler et al. 2000), respectively. P7 also underwent *ortho*-cleavage to form 2-carboxycinnamic acid (P10), which was then converted to phthalic acid (P12). To our knowledge, this pathway (from P7 to P12) in *Burkholderia* species has not been previously reported. Annweiler et al. (2000) proposed a possible conversion of naphthalene-1,2-diol (P7) to 2-carboxycinnamic acid (P10) by *ortho*-cleavage. Transformation of P7 to P10 by this strain represented the first observation of *ortho*-cleavage of two rings-PAH-diols by Gram-negative bacteria In general, hydratase–aldolase catalyzes *o*-hydroxy- or *o*-carboxybenzalpyruvic acids to salicylaldehyde or 2-carboxybenzaldehyde correspondingly. Eaton & Chapman (1992) reported that hydratase–aldolase could not attack *o*-hydroxycinnamic acid. This suggested that a different enzyme be involved in the conversion of 2-carboxycinnamic acid (P10) to phthalic acid (P12). It is interesting to note a general trend that the metabolites above P7 (i.e., P1-5 except P6) reached a maximum concentration at day 7 or earlier (upper catabolism pathways) while the metabolites below P7 (i.e., P8–13) peaked at day 7 or later (lower catabolism pathways). It may be interpreted as that the catabolism rate of P7 may be alleviated after 7 days.

In summary, detection and identification of 13 metabolites show that *Burkholderia* sp. C3 can degrade phenanthrene. A positive correlation between phenanthrene degradation and cell growth supports that *Burkholderia* sp. C3 can utilize phenanthrene a sole carbon source. Phenanthrene degradation by the strain C3 starts from dioxygenation at 1,2- and 3,4- positions. The two pathways are converged in naphthalene-1,2-diol. This diol is further metabolized by novel *ortho*-cleavage to produce phthalate through 2-carboxycinnamic acid, and common *meta*-cleavage to produce gentisic acid through 2-hydroxybenzalpyruvic acid and salicylate.

Acknowledgements

This work was supported in part by US-EPA award no. 989512-01-1 and USDA-TSTAR Grants 00-34135-9576, 2001-34135-11295, and 2002-34135-12724.

References

Altschul SF, Madden TL, Schäffer AA, Zhang J, Zhang Z, Miller W & Lipman DJ (1997) Gapped BLAST and PSI-BLAST: a new generation of protein database search programs. Nucleic Acids Res. 25: 3389–3402

Annweiler E, Richnow HH, Antranikian G, Hebenbrock S, Garms C, Franke S, Francke W & Michaelis W (2000) Naphthalene degradation and incorporation of naphthalene derived carbon into biomass by the thermophile *Bacillus thermoleovorans*. Appl. Environ. Microbiol. 66: 518–523

Balashova NV, Kosheleva IA, Golovchenko NP & Boronin AM (1999) Phenanthrene metabolism by *Pseudomonas* and *Burkholderia* strains. Process Biochem. 35: 291–296

Balashova NV, Stolz A, Knackmuss H-J, Kosheleva IA, Naumov AV & Boronin AM (2001) Purification and

characterization of a salicylate hydroxylase involved in 1-hydroxy-2-naphthoic acid hydroxylation from the naphthalene and phenanthrene-degrading bacterial strain *Pseudomonas putida* BS202-P1. Biodegradation 12: 179–188

Bastiaens L, Springael D, Wattiau P, Harms H, deWachter R, Verachtert H & Diels L (2000) Isolation of adherent polycyclic aromatic hydrocarbon (PAH)-degrading bacteria using PAH-sorbing carriers. Appl. Environ. Microbiol. 66: 1834–1843

Camara B, Herrera C, Gonzalez M, Couve E, Hofer B & Seeger M (2004) From PCBs to high toxic metabolites by the biphenyl pathway. Environ. Microbiol. 6: 842–850

Canada KA, Iwashita S, Shim H & Wood TK (2002) Directed evolution of toluene *ortho*-monooxygenase for enhanced 1-naphthol synthesis and chlorinated ethane degradation. J. Bacteriol. 183: 344–349

Dean-Ross D, Moody J & Cerniglia CE (2002) Utilization of mixtures of polycyclic aromatic hydrocarbons by bacteria isolated from contaminated sediment. FEMS Microbiol. Ecol. 41: 1–7

Eaton RW & Chapman PJ (1992) Bacterial metabolism of naphthalene: construction and use of recombinant bacteria to study cleavage of 1,2-dihydroxynaphthalene and subsequent reactions. J. Bacteriol. 174: 7542–7554

Gibson DT & Parales RE (2000) Aromatic hydrocarbon dioxygenases in environmental biotechnology. Curr. Opin. Biotechnol. 11: 236–243

Johnsen AR, Wick LY & Harms H (2005) Principles of microbial PAH-degradation in soil. Environ. Pollut. 133: 71–84

Johnson GR, Jain RK & Spain JC (2000) Properties of the trihydroxytoluene oxygenase from *Burkholderia cepacia* R34: extradiol dioxygenase from the 2,4-dinitrotoluene pathway. Arch. Microbiol. 173: 86–90

Juhasz AL, Britz ML & Stanley GA (1997) Degradation of fluoranthene, pyrene, benz[*a*]anthracene and dibenz[*a*,*h*]anthracene by *Burkholderia cepacia*. J. Appl. Microbiol. 83: 189–198

Juhasz AL, Stanley GA & Britz ML (2000) Microbial degradation and detoxification of high molecular weight polycyclic aromatic hydrocarbons by *Stenotrophomonas maltophilia* strain VUN 10,003. Lett. Appl. Microbiol. 30: 396–401

Kang H, Hwang SY, Kim YM, Kim E, Kim YS, Kim SK, Kim SW, Cerniglia CE, Shuttleworth KL & Zylstra GJ (2003) Degradation of phenanthrene and naphthalene by a *Burkholderia* species strain. Can. J. Microbiol. 49: 139–144

Keum YS, Seo JS & Li QX (2005) Synthesis of bacterial metabolites of polycyclic aromatic hydrocarbons: Benzochromenones, *o*-carboxyvinylnaphthoates, and *o*-substituted aryl-α-oxobutenoates. Synth. Commun. 35: 2685–2693

Keum YS, Seo JS, Hu Y & Li QX (2006 in press) Degradation pathways of phenanthrene by *Sinorhizobium* sp. C4. Appl. Microbiol. Biotechnol. (DOI 10.1007/s00253–005–0219-z)

Kim TJ, Lee EY, Kim YJ, Cho KS & Ryu HW (2003) Degradation of polyaromatic hydrocarbons by *Burkholderia cepacia* 2A-12. World J. Microbiol. Biotechnol. 19: 411–417

Kim YH, Freeman JP, Moody JD, Engesser KH & Cerniglia CE (2005) Effects of pH on the degradation of phenanthrene and pyrene by *Mycobacterium vanbaalenii* PYR-1. Appl. Microbiol. Biotechnol 67: 275–285

Krivobok S, Kuony S, Meyer C, Louwagie M, Willison JC & Jouanneau Y (2003) Identification of pyrene-induced proteins in *Mycobacterium* sp. strain 6PY1: evidence for two ring-hydroxylation dioxygenases. J. Bacteriol. 185: 3828–3841

Lane DJ (1991) 16S/23S rRNA sequencing. In: Stackebrant E & Goodfellow M. (Eds) Nucleic Acid Techniques in Bacterial Systematics (pp. 115–175). John Wiley & Sons, Chichester

Marmur J (1961) A procedure for the isolation of deoxyribonucleic acid from microorganisms. J. Mol. Biol. 3: 208–218

Moody JD, Freeman JP, Doerge DR & Cerniglia CE (2001) Degradation of phenanthrene and anthracene by cell suspensions of *Mycobacterium* sp. strain PYR-1. Appl. Environ. Microbiol. 67: 1476–1483

Parales RE, Mesnick SM, Yu CL, Boyd DR, Sharma ND & Gibson DT (2000) Regiospecificity and enantioselectivity of naphthalene dioxygenase during arene *cis*-dihydroxylation: Control by phenylalanine 352 in the α subunit. J. Bacteriol. 182: 5495–5504

Pinyakong O, Habe H, Supaka N, Pinpanichkarn P, Juntongjin K, Yoshida T, Furihata K, Nojiri H, Yamane H & Omori T (2000) Identification of novel metabolites in the degradation of phenanthrene by *Sphingomonas* sp. strain P2. FEMS Microbiol. Lett. 191: 115–121

Prabhu Y & Phale PS (2003) Biodegradation of phenanthrene by *Pseudomonas* sp. strain PP2: novel metabolic pathway, role of biosurfactant and cell surface hydrophobicity in hydrocarbon assimilation. Appl. Microbiol. Biotechnol. 61: 342–351

Samanta SK, Chakraborti AK & Jain RK (1999) Degradation of phenanthrene by different bacteria: evidence for novel transformation sequences involving the formation of 1-naphthol. Appl. Microbiol. Biotechnol. 53: 98–107

Stingley RL, Khan AA & Cerniglia CE (2004) Molecular characterization of a phenanthrene degradation pathway in *Mycobacterium vanbaalenii* PYR-1. Biochem. Biophys. Res. Commun. 322: 133–146

van Herwijnen R, van de Sande BF, van der Wielen FWM, Springael D, Govers HAJ & Parsons JR (2003) Influence of phenanthrene and fluoranthene on the degradation of fluorene and glucose by *Sphingomonas* sp. strain LB126 in chemostat cultures. FEMS Microbiol Ecol 46: 105–111